Original Article

Quantitative assessment of crystal dissolution in gout during urate-lowering therapy with computer-aided MicroPure imaging: a cohort study

Qiao Wang[1,2,3,4#], Hui Bao[5#], Le-Hang Guo[1,2,3,4^], Feng-Shan Jin[2,3,4], Xiao-Long Li[2,3,4], Hao-Hao Yin[2,3,4], Wen-Wen Yue[2,3,4], An-Qi Zhu[1,2,3,4], Li-Fan Wang[1,2,3,4], Li-Ping Sun[2,3,4], Hui-Xiong Xu[1,2,3,4^]

[1]Department of Medical Ultrasound, Shanghai Skin Disease Hospital, School of Medicine, Tongji University, Shanghai, China; [2]Department of Medical Ultrasound & Tumor Minimally Invasive Treatment, Shanghai Tenth People's Hospital, Shanghai, China; [3]Ultrasound Research and Education Institute, Clinical Research Center for Interventional Medicine, School of Medicine, Tongji University, Shanghai Engineering Research Center of Ultrasound Diagnosis and Treatment, Shanghai, China; [4]National Clinical Research Center for Interventional Medicine, Shanghai, China; [5]Department of Nephrology and Rheumatology, Shanghai Tenth People's Hospital, School of Medicine, Tongji University, Shanghai, China

Contributions: (I) Conception and design: All authors; (II) Administrative support: LP Sun, HX Xu, H Bao, LH Guo; (III) Provision of study materials or patients: Q Wang, H Bao, LH Guo, FS Jin; (IV) Collection and assembly of data: Q Wang, WW Yue, HH Yin, XL Li; (V) Data analysis and interpretation: Q Wang, XL Li, AQ Zhu, LF Wang, FS Jin; (VI) Manuscript writing: All authors; (VII) Final approval of manuscript: All authors.

[#]These authors contributed equally to this work.

Correspondence to: Le-Hang Guo, MD, PhD. Department of Medical Ultrasound, Shanghai Skin Disease Hospital, Shanghai Tenth People's Hospital, Ultrasound Research and Education Institute, Shanghai Engineering Research Center of Ultrasound Diagnosis and Treatment, School of Medicine, Tongji University, 1278 Baode Road, Shanghai 200443, China. Email: gopp1314@hotmail.com; Li-Ping Sun, MD, PhD. Department of Medical Ultrasound, Shanghai Tenth People's Hospital, Ultrasound Research and Education Institute, Shanghai Engineering Research Center of Ultrasound Diagnosis and Treatment, School of Medicine, Tongji University, 301 Yanchangzhong Road, Shanghai 200072, China. Email: sunliping_s@126.com.

Background: To evaluate whether MicroPure imaging, an ultrasound (US) image-processing technique with computer-aided analysis, can quantitatively detect crystal dissolution during urate-lowering therapy (ULT) in gout.

Methods: This was a prospective study of gout patients requiring ULT. The first metatarsophalangeal joints were examined using US and MicroPure before and after 3 months of ULT. Elementary lesions of gout, including the double contour sign (DCS), aggregates, tophi, erosion, and other US features were recorded at baseline and 3 months. MicroPure imaging features were automatically calculated by a self-developed software. Patients were divided into goal-achieved and goal-not-achieved groups according to their urate levels at 3 months. The US and MicroPure imaging features of the two groups were analyzed at baseline and 3 months.

Results: A total of 55 consecutive patients were enrolled (25: goal-achieved group; 30: goal-not-achieved group). US findings demonstrated that the power Doppler signal grade decreased at 3 months, regardless of the group (both $P<0.05$). From baseline to 3 months, tophi size and the DCS reduced in the goal-achieved group (both $P<0.05$), while the US aggregate features showed no difference ($P=0.250$). However, on the MicroPure imaging, the number and density of aggregates at 3 months decreased in the goal-achieved group (both $P<0.05$). There were no significant changes at 3 months in any of the MicroPure imaging features in the goal-not-achieved group (all $P>0.05$).

Conclusions: In comparison with B-mode US, computer-aided MicroPure imaging can sensitively and quantitatively detect aggregate dissolution during effective ULT after only 3 months of treatment.

Keywords: Gout; ultrasound; follow-up; MicroPure imaging; quantification

^ ORCID: Le-Hang Guo, 0000-0002-5685-1280; Hui-Xiong Xu, 0000-0002-8699-854X.

Submitted Jul 16, 2021. Accepted for publication Sep 10, 2021.
doi: 10.21037/atm-21-4059
View this article at: https://dx.doi.org/10.21037/atm-21-4059

Introduction

Gout is caused by prolonged hyperuricemia, characterized by the deposition of monosodium urate (MSU) crystals in the joints and soft tissues (1). It is the most common form of inflammatory arthritis in adults, with a prevalence of 3.9% in the United States, 1.4–2.5% in the United Kingdom, and 1–2% in China (2,3).

If untreated, polyarticular attacks and joint deformities may occur, and the condition is associated with cardiovascular and kidney diseases (4). Therefore, early treatment is essential. Urate-lowering therapy (ULT) is based on promoting urate excretion or reducing uric acid production to reduce serum urate levels and further prevent gout flares. ULT is a cornerstone of gout treatment (5,6). The treat-to-target approach of ULT (serum urate levels <360 μmol/L) is recommended for gout patients receiving ULT (7). However, patients' adherence to ULT remains poor (8,9). Ultrasound (US) and dual-energy CT (DECT) can be used to detect crystal depositions and are recommended by the American College of Rheumatology (ACR) and the European League Against Rheumatism (EULAR) for the diagnosis of gout (3,10). DECT can identify and quantify the MSU crystal deposition. However, it has the disadvantages of time consuming, expensive and radiation. Therefore, US is favored by clinicians.

The Outcome Measures in Rheumatology (OMERACT) ultrasound working group defined four elementary lesions in gout: aggregates, the double contour sign (DCS), tophi, and erosion (11).

Several studies have shown that ultrasound-detected crystal depositions gradually decrease and reduce tophi size during efficient ULT (12-14). However, to our knowledge, there are only two recent studies that have reported a scoring system to quantify changes in aggregates, erosion, and the DCS (15,16). These studies demonstrated that US-detected urate crystal depositions were reduced during effective ULT, thus encouraging clinicians and gout patients to persist in the treat-to-target approach of ULT (15,16). However, the scoring system for elementary lesions is semiquantitative and may be subjective. Therefore, a convenient and non-radiative method for objectively and quantitatively monitoring urate crystal dissolution during ULT is needed.

It is well-established that tophi size is quantifiable, but a tophus is often only apparent in patients with a lengthy disease history (17). The DCS and erosion are difficult to quantify. Aggregates appear as echogenic spots on B-mode US and can be found in most gout patients, making them the optimal lesions for quantification. However, the visualization of aggregates on B-mode US is affected by speckle noise and surrounding tissues. MicroPure imaging (Toshiba America Medical Systems, Tustin, CA, USA) is a commercial US image-processing technology. It can filter the background to highlight tiny reflectors and separate them from artifacts (18). MicroPure imaging has been used to identify microcalcifications in breast tissue and was initially used to display urate crystals in gout (19,20). Therefore, it might be feasible to use MicroPure to monitor aggregate dissolution during ULT. In the previous study, investigators calculated the number of aggregates by the naked eyes, the method is time consuming and subjective (20). To quantitatively and objectively assess the changes in aggregates using MicroPure imaging, a self-developed image analysis software was developed in the present study.

The primary aim of this pilot study was to explore the value of MicroPure imaging with computer-aided analysis in quantitatively monitoring aggregate dissolution during ULT in gout. The secondary aim was to evaluate the inflammatory changes in the joints during ULT.

We present the following article in accordance with the STROBE reporting checklist (available at https://dx.doi.org/10.21037/atm-21-4059).

Methods

Study groups

The cohort study was approved by the ethics committee of the Tenth People's Hospital Affiliated to Tongji University (Approval No.: SHSY-IEC-KY-4.0/18-170/01). Our database was prospectively established, and all patients provided informed consent. All procedures performed in this study involving human participants were in accordance with the Declaration of Helsinki (as revised in 2013).

Patients were recruited from October 2019 to July 2020.

Consecutive patients from the university hospital with joint symptoms were evaluated by a physician, and then patients with clinically suspected gout subsequently underwent routine US examinations. We followed up the serum urate level, visual analog score (VAS), and US features. The last follow-up date was October 2020. The number of cases in the study period determined the sample size.

Inclusion criteria were as follows: (I) a diagnosis of gout according to the 2015 Gout Classification Criteria of the ACR/EULAR (3); (II) >18 years of age; (III) the first metatarsophalangeal joint was attacked; (IV) ULT was required [ULT is initiated for patients with any of the following conditions: frequency of gout flares ≥2 annually, ≥1 subcutaneous tophus, or evidence of radiographic damage (any modality) attributable to gout] (7); and (V) no ULT in the previous 6 months. Exclusion criteria were as follows: (I) patients who did not adhere to ULT; (II) patients with osteoarthritis, rheumatoid arthritis, or psoriatic arthritis.

According to the 2015 Gout Classification Criteria of the ACR/EULAR, a case was regarded as a typical episode if two of the following three conditions were met: (I) time to maximal pain <24 h; (II) resolution of symptoms in ≤14 days; (III) complete resolution between symptomatic episodes. One typical episode was scored as 1 point, whereas recurrent typical episodes were scored as 2 points. Erythema overlying the joint, inability to bear touch or pressure on the joint, and difficulty walking were each scored as 1 point. If the serum urate level <240 μmol/L, 4 points were subtracted; no points were scored if the serum urate level was 240–360 μmol/L; 2 points were scored if the serum urate level was 360–480 μmol/L; 3 points were scored if the serum urate level was 480–600 μmol/L; 4 points were scored if the serum urate level was ≥600 μmol/L. The threshold score for diagnosing gout was ≥8 points (3).

Demographic and clinical data, including sex, age, disease duration, serum urate level, and VAS were recorded at baseline.

Treatment and follow-up

For acute gout flares, the colchicine regimen (1.0 mg immediately followed by 0.5 mg an hour later, and then maintaining 0.5 mg/bid until the flare resolves) was used. Benzbromarone (Excella GmbH & Co. KG, Nurnberger, Germany) and febuxostat (Wanbang, Jiangsu, China) were used to lower the urate level. The starting doses of benzbromarone and febuxostat were 25 and 40 mg/d, respectively. The physician followed up all patients monthly to assess the urate level; if the urate levels were >360 μmol/L, the dose of benzbromarone was increased by 25 mg (maximum dosage ≤100 mg), and the dose of febuxostat was increased by 40 mg (maximum dosage ≤120 mg). The medication and dosage were decided by the physician.

Although allopurinol is recommended as the first-line agent by the ACR and EULAR, it is associated with severe cutaneous adverse reactions (21). Evidence has shown that the HLA-B*5801 allele can portend a higher risk of severe cutaneous adverse reactions, with the highest prevalence (7.4%) in Han Chinese individuals (22), which limits the application of allopurinol.

According to the EULAR/ACR recommendations, the target of ULT was a serum urate level <360 μmol/L (7,23). Patients were followed up for 3 months and divided into goal-achieved and goal-not-achieved groups based on their serum urate level at 3 months (*Figure 1*).

US examinations at baseline and follow-up

Patients underwent B-mode US, power Doppler US (PDUS), and MicroPure examinations at baseline and 3 months. All US examinations were performed by one radiologist (L.H.G., 8 years' experience in musculoskeletal US) using an Aplio 500 TUS-A500 (Toshiba Medical Systems Corporation, Tochigi, Japan) with an 18-MHz linear probe. The radiologist was not blinded to the patients' clinical symptoms but was blinded to the serum urate levels at baseline and 3 months.

All US examinations were performed according to standardized guidelines (24). The affected first metatarsophalangeal joint was observed from the lateral, dorsal, and plantar views on both the longitudinal and transverse axes. Toes were flexed to view a wider portion of the hyaline cartilage in the dorsal view. The frequency, depth, gain, and focus were adjusted for clarity, and the PDUS images were adjusted to display the Doppler flow signals without noise artifacts. The radiologist assessed the affected joint and measured the maximum synovial thickness and the longest diameter of tophi if present.

MicroPure images were then obtained in the longitudinal plane with the maximum synovial thickness. The radiologist manually traced the profile of the synovium to define the region of interest (ROI) on the still MicroPure image (*Figure 2*). All the B-mode US, PDUS, and MicroPure

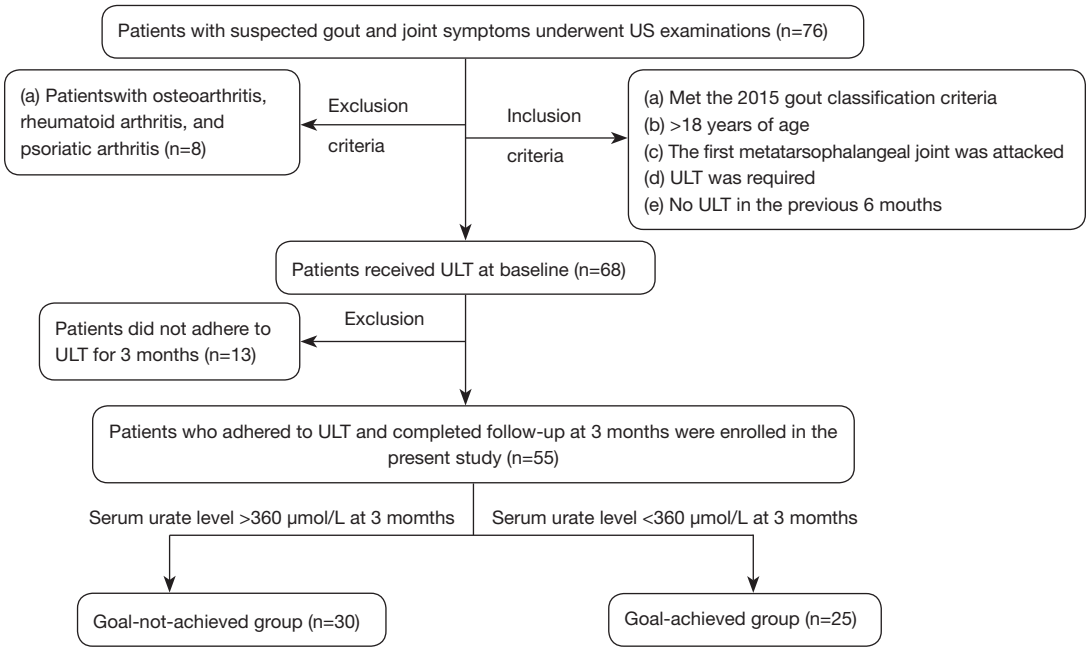

Figure 1 Flowchart of patient selection in this prospective study. ULT, urate-lowering therapy.

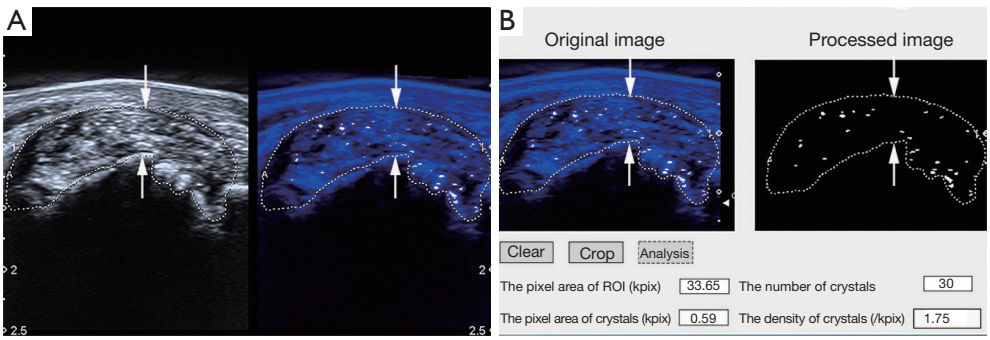

Figure 2 The process of quantitative MicroPure imaging with computer-aided analysis. (A) The traced profile of the synovium on a still MicroPure image defines the ROI (arrows). (B) A self-developed software is used to calculate the number, density, and pixel area of aggregates and the pixel area of ROI (arrows). ROI, region of interest.

images were stored on a hard disk for further analysis.

Image interpretation

To mitigate subjective bias, the B-mode US and PDUS images were reviewed by two independent radiologists (F.S.J. and X.L.L., 10 and 6 years' experience in musculoskeletal US, respectively) who were blinded to the patients' symptoms, results of previous examinations, and clinical histories.

The radiologists noted the presence of elementary lesions and joint cavity effusion at baseline and 3 months. The International Consensus for Ultrasound Lesions in Gout were used (25), aggregates were defined as small hyperechoic crystal deposits in the synovium or in the effusion, the DCS was defined as crystal deposits on the surface of the cartilage, tophi were defined as large aggregates of crystals, erosion was defined as discontinuity of the bone surface visible in two perpendicular planes, and joint cavity effusion was defined as the compressible anechoic region (*Figure 3*). The radiologists also evaluated the power Doppler flow signal in the synovium using a

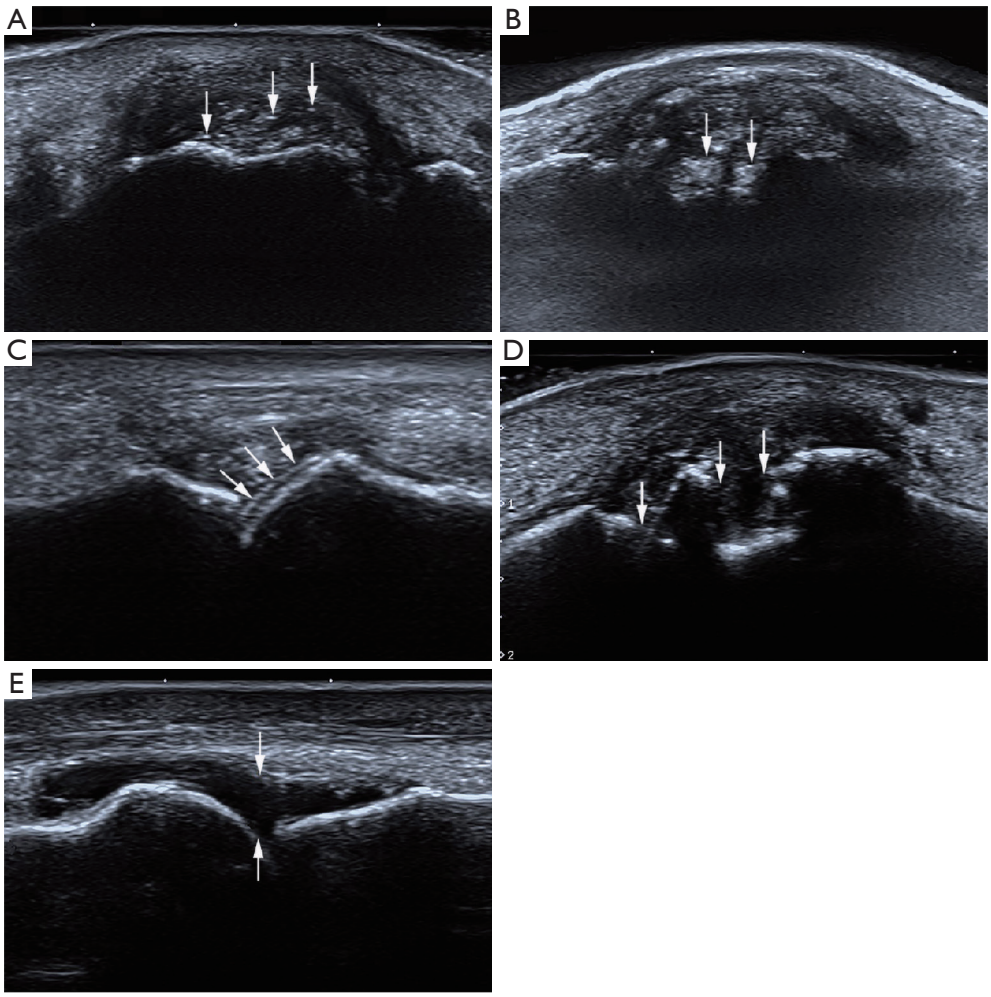

Figure 3 Longitudinal plane of B-mode US features in the first metatarsophalangeal joint. (A) Aggregates (arrows); (B) tophi (arrows); (C) double-contour sign (arrows); (D) cortical bone erosions (arrows); (E) joint cavity effusion (arrows).

semiquantitative grade: (I) grade 0= no color signal; (II) grade 1= single vessel signal; (III) grade 2= confluent color signals in less than half of the area of the synovium; (IV) grade 3= confluent color signals in more than half of the area of the synovium (26) (*Figure 4*). Discrepancies were resolved through discussion. The consistent results were used for further analysis. The radiologists repeated the interpretation one month later to test the inter- and intraobserver agreement of the US features.

MicroPure imaging with computer-aided analysis

The aggregates in the ROI were conveniently digitalized as pixels by a self-developed program in MATLAB (Mathworks, Natick, MA). The number, density, and pixel area of the aggregates and the pixel area of the ROI can be automatically output by the software (*Figure 2*). It should be noted that there were still some crystal-like noise artifacts on the MicroPure imaging. Thus, before the study began, the sensitivity of the program was calibrated to eliminate the artifacts. Theoretically, images of normal joints will not have a crystal-like appearance. Twenty volunteers who had never had joint pain and hyperuricemia were recruited before the study commenced. MicroPure images were obtained of the volunteers' first metatarsophalangeal joint. The images were then imported into the software, and the program's sensitivity was adjusted until there were no crystal-like appearances. The designed pixel-counting strategy provided a proof of concept for quantifying the urate crystals in US.

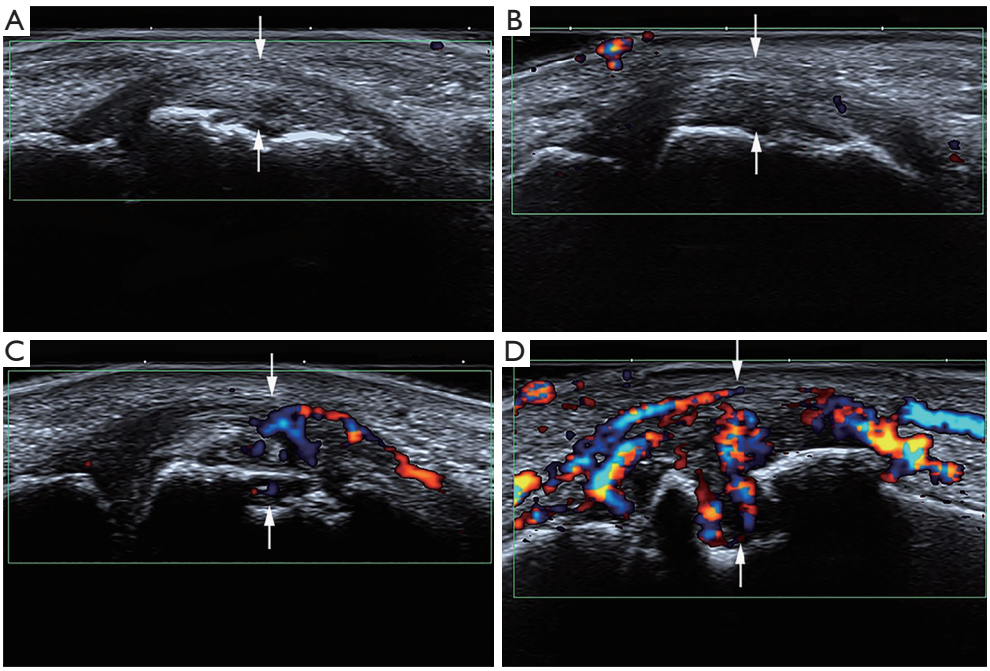

Figure 4 Power Doppler flow signal grade of the longitudinal plane. (A) Grade 0 (arrows); (B) Grade 1 (arrows); (C) Grade 2 (arrows); (D) Grade 3 (arrows).

To test the inter- and intraoperator reproducibility of the MicroPure imaging, another 20 gout patients were examined by two operators (L.F.W. and A.Q.Z.) with 3 years' experience in musculoskeletal US. The protocols for obtaining the MicroPure image and tracing the profile of the synovium to define the ROI were as previously described. The images traced by the operators were analyzed by the software, and the results were recorded. The data was only used for the reproducibility assessment.

Statistical analyses

Statistical analyses were completed using SPSS (version 20.0; SPSS, Chicago). Normal distributions were evaluated using the Kolmogorov-Smirnov test. Patients with missing data or who were lost to follow-up were excluded. As samples did not follow a normal distribution in the present study, results are expressed as medians and interquartile ranges (IQR). Clinical data and quantitative US features between the groups were compared using the Mann-Whitney U test. For qualitative US features, the chi-squared test or Fisher's exact test was used for comparisons between the two groups. The McNemar test was used for comparisons between baseline and 3 months. The clinical data, quantitative US features, and MicroPure imaging features at baseline and 3 months were compared using the nonparametric Wilcoxon signed-rank test. A two-tailed P value of <0.05 was considered statistically significant.

The Cohen κ test was performed to test observer reproducibility when evaluating US features. The intraclass correlation coefficient (ICC) was calculated to test the inter- and intraoperator reproducibility of the MicroPure images. Agreement was rated as poor (ICC, 0.00–0.20), fair (ICC, 0.20–0.40), good (ICC, 0.40–0.75), or excellent (ICC >0.75) (27).

Results

Patient characteristics

A total of 68 gout patients received ULT in the present study. Of these, 13 patients failed to adhere to ULT for 3 months due to a lack of awareness of the importance of ULT. Therefore, a final number of 55 gout patients (5 women, 50 men) were included in the present study. Of these, 25 patients were categorized as the goal-achieved group and 30 as the goal-not-achieved group (*Figure 1*). The median age of all patients was 58.0 years (IQR: 40.5–67.8 years), and the median disease duration was 48.0 months (IQR:

Table 1 Patient characteristics at baseline

Characteristics	Goal-achieved group	Goal-not-achieved group	P value
No. of patients	25	30	
No. of joints	25	30	
Patient sex			0.65
Men	22	28	
Women	3	2	
Age (years)*	62.0 (59.0–69.0)	55.0 (35.0–65.5)	0.051
Disease duration (months)*	48.0 (21.0–180.0)	48.0 (18.0–150.0)	0.978
VAS (scores)*	7.0 (3.0–9.0)	6.5 (3.3–9.5)	0.928
Serum urate level (μmol/L)*	538.6 (473.2–588.8)	523.6 (470.6–567.2)	0.372

Data are number of patients or joints unless indicated otherwise. *, except for P values, data are medians, with interquartile ranges (IQR) in parentheses. VAS, visual analog score.

21.0–180.0 months). Benzbromarone was used for 24 patients, and febuxostat was used for 31 patients.

The following clinical data showed no significant differences between the goal-achieved group and the goal-not-achieved group at baseline: sex, age, disease duration, VAS, and serum urate levels (all P>0.05) (*Table 1*).

From baseline to 3 months, the VAS in both the goal-achieved and goal-not-achieved groups decreased significantly (both P=0.005). The serum urate levels decreased from 538.6 μmol/L (IQR: 473.2–588.8 μmol/L) to 325.3 μmol/L (IQR: 291.9–340.6 μmol/L) (P=0.001) in the goal-achieved group, and from 523.6 μmol/L (IQR: 470.6–567.2 μmol/L) to 449.1 μmol/L (IQR: 385.3 –529.2 μmol/L) (P=0.002) in the goal-not-achieved group.

US features at baseline and follow-up

None of US features showed a significant difference at baseline between the two groups, except joint cavity effusion (P=0.027) (*Table 2*).

In the goal-achieved group, aggregates were present in 100% of the patients at baseline, decreasing to 88.0% of the patients at 3 months (P=0.250). The DCS was present in 36.0% of the patients at baseline, decreasing to 12.0% at 3 months (P=0.031). From baseline to 3 months, tophi did not disappear on the B-mode US, but the tophi size significantly decreased from 4.6 mm (IQR: 3.85–5.6 mm) to 2.6 mm (IQR: 2.45–4.0 mm) (P=0.043). Cortical bone erosion appeared in 40.0% of patients at baseline, and it was observed in three additional patients at 3 months (P=0.250). Joint cavity effusion presented in 4.0% of the patients at baseline and had disappeared at 3 months. From baseline to 3 months, the synovium thickness decreased from 5.1 mm (IQR: 4.3–5.8 mm) to 4.5 mm (IQR: 3.9–5.4 mm) (P=0.016). Further, PDUS decreased from 1.0 (IQR: 1.0–2.0) to 0.0 (IQR: 0.0–1.0) (P=0.005) (*Figure 5*).

In the goal-not-achieved group, there were no changes in the following US features from baseline to 3 months: aggregates, DCS, tophi, and cortical bone erosion. Tophi size did not show a significant difference between baseline and 3 months [4.55 mm (IQR: 3.2–5.6 mm) *vs.* 4.35 mm (IQR: 2.75–5.2 mm)] (P=0.255). Joint cavity effusion presented in 26.7% of the patients at baseline, decreasing to 6.7% at 3 months (P=0.031). From baseline to 3 months, the synovium thickness decreased from 5.3 mm (IQR: 4.2–6.1 mm) to 4.7 mm (IQR: 3.4–5.6 mm) (P=0.003). PDUS decreased from 2.0 (IQR: 1.0–2.0) to 0.0 (IQR: 0.0–2.0) (P<0.0001) (*Figure 5*).

Computer-aided MicroPure imaging features at baseline and follow-up

At baseline, the MicroPure imaging data output by the computer-aided system showed no significant differences between the two groups (all P>0.05) (*Table 2*).

In the goal-achieved group, from baseline to 3 months, the number of aggregates was significantly lower [9.0 (IQR: 5.0–15.5) *vs.* 8.0 (IQR: 3.5–15.0)] (P=0.024). In addition, the density of aggregates was also significantly lower [4.35/kpix (IQR: 2.87–6.61/kpix) *vs.* 3.52/kpix (IQR: 1.75–7.26/kpix)] (P=0.047). However, the pixel area of the ROI and the pixel area of the aggregates did not show significant decreases at

Table 2 US and MicroPure imaging features at baseline in the goal-achieved and goal-not-achieved groups

Features	Goal-achieved group (n=25)	Goal-not-achieved group (n=30)	P value
B-mode features			
Thickness of synovium (mm)	5.1 (4.3–5.8)	5.3 (4.2–6.1)	0.719
Aggregates^, n (%)	25 (100.0)	30 (100.0)	1.000
DCS^, n (%)	9 (36.0)	5 (16.7)	0.654
Cortical bone erosion^, n (%)	10 (40.0)	16 (53.3)	0.908
Joint cavity effusion^, n (%)	1 (4.0)	8 (26.7)	0.027*
Tophi^, n (%)	6 (24.0)	12 (40.0)	0.341
PDUS	1.0 (1.0–2.0)	2.0 (1.0–2.0)	0.438
MicroPure imaging features			
Number of aggregates	9.0 (5.0–15.5)	10.0 (5.0–19.0)	0.420
Density of aggregates (/kpix)	4.35 (2.87–6.61)	4.78 (3.01–11.59)	0.814
Pixel area of aggregates (kpix)	0.23 (0.05–0.34)	0.17 (0.09–0.43)	0.824
Pixel area of ROI (kpix)	43.90 (27.72–54.41)	38.98 (29.19–52.67)	0.665

Data are median, with interquartile ranges (IQR) in parentheses except where indicated. ^, data are number of patients, with percentages in parentheses; *, indicates a significant difference between the two groups (P<0.05). DCS, double-contour sign; PDUS, power Doppler ultrasound; ROI, region of interest; US, ultrasound.

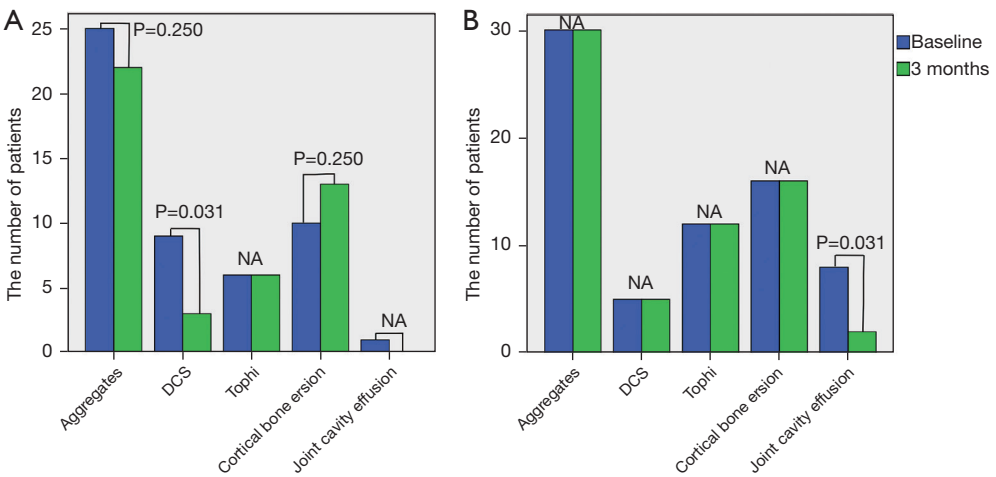

Figure 5 Changes in B-mode US features of gout at baseline and 3 months after urate-lowing therapy in the goal-achieved group (A) and the goal-not-achieved group (B). DCS, double contour sign.

3 months (both P>0.05) (*Table 3*).

In the goal-not-achieved group, the following features did not show significant differences from baseline to 3 months: the number of aggregates, the density of aggregates, the pixel area of the ROI, and the pixel area of the aggregates (all P>0.05) (*Table 3*).

Reproducibility

There was excellent intraoperator reproducibility of the MicroPure image, and interoperator reproducibility was good. The intra- and interobserver reproducibility were high for the US features (*Table 4*).

Table 3 Comparisons of clinical data and MicroPure imaging features between baseline and 3 months of ULT for the two groups

Parameter	Goal-achieved group (n=25)			Goal-not-achieved group (n=30)		
	Baseline	3 months	P value	Baseline	3 months	P value
Clinical data						
VAS score	7.0 (3.0–9.0)	0.0 (0.0–2.5)	0.005*	6.5 (3.5–9.5)	0.0 (0.0–2.0)	0.005*
Serum urate level (μmol/L)	538.6 (473.2–588.8)	325.3 (291.9–340.6)	0.001*	523.6 (470.6–567.2)	449.1 (385.3–529.2)	0.002*
MicroPure imaging features						
Number of MSU crystals	9.0 (5.0–15.5)	8.0 (3.5–15.0)	0.024*	10.0 (5.0–19.0)	10.0 (3.0–14.0)	0.485
Density of MSU crystals (/kpix)	4.35 (2.87–6.61)	3.52 (1.75–7.26)	0.047*	4.78 (3.01–11.59)	4.31 (1.65–6.95)	0.090
Pixel area of MSU crystals (kpix)	0.23 (0.05–0.34)	0.17 (0.07–0.53)	0.140	0.17 (0.09–0.43)	0.13 (0.06–0.33)	0.370
Pixel area of ROI (kpix)	43.90 (27.72–54.41)	40.05 (24.66–44.89)	0.112	38.98 (29.19–52.67)	32.48 (21.81–45.61)	0.107

Data are median, with interquartile ranges (IQR) in parentheses except where indicated. *, indicates a significant difference between baseline and 3 months in the two groups (P<0.05). ULT, urate-lowering therapy; VAS, visual analog score.

Table 4 Reproducibility of US and MicroPure imaging features

Reproducibility	Intra-		Inter-
	Reader/operator 1	Reader/operator 2	Readers/operators 1 and 2
US features (readers)			
Aggregates*	0.876 (0.509–1.000)	0.896 (0.697–1.000)	0.831 (0.309–1.000)
DCS*	0.871 (0.581–1.000)	0.933 (0.680–1.000)	0.938 (0.673–1.000)
Cortical bone erosion*	0.909 (0.779–0.998)	0.954 (0.821–1.000)	0.908 (0.813–1.000)
Joint cavity effusion*	0.944 (0.835–1.000)	0.879 (0.700–0.976)	0.721 (0.277–0.905)
Tophi*	0.845 (0.708–0.975)	0.788 (0.601–0.935)	0.788 (0.381–1.000)
PDUS*	0.936 (0.773–1.000)	0.937 (0.848–1.000)	0.874 (0.728–0.967)
MicroPure imaging features (operators)			
Number of aggregates^	0.987 (0.970–0.995)	0.993 (0.983–0.997)	0.879 (0.715–0.949)
Density of aggregates^	0.993 (0.843–0.972)	0.904 (0.763–0.961)	0.681 (0.247–0.865)
Pixel area of aggregates^	0.968 (0.925–0.987)	0.985 (0.962–0.994)	0.874 (0.727–0.945)
Pixel area of ROI^	0.982 (0.959–0.987)	0.994 (0.985–0.998)	0.819 (0.572–0.923)

Numbers in parentheses are 95% CIs. *, data are kappa values; ^, data are intraclass correlation coefficients for MicroPure imaging. US, ultrasound; DCS, double-contour sign; PDUS, power Doppler ultrasound; ROI, region of interest.

Discussion

US is a useful modality in the diagnosis and follow-up of gout. In the present study, all gout patients were followed up for 3 months during ULT, and the OMERACT definitions for elementary lesions in gout were adopted. Compared with conventional US, computer-aided MicroPure imaging can realize the quantification of aggregates. In addition, computer-aided analysis is objective.

Our study found that MicroPure imaging with computer-aided analysis quantitatively showed that the number and density of aggregates significantly decreased at 3 months in the goal-achieved group. However, qualitative B-mode US aggregate features did not show a significant decrease in the goal-achieved group. The results indicate that computer-aided MicroPure imaging can detect aggregate dissolution

more sensitively than qualitative B-mode US. In other words, the aggregates are still showing as present on the B-mode US even though the aggregate load is decreased. Hammer *et al.* suggested that aggregates show a smaller decrease on B-mode US because large tophi will dissolve into smaller aggregates during effective ULT (15). We speculated that the rate of aggregate dissolution is higher than the rate of generation during effective ULT.

Qualitative B-mode US DCS features decreased in the goal-achieved group, implying that the DCS is sensitive to change during effective ULT, consistent with previous studies (14,15,28). A tophus is characterized by foreign body granulomas consisting of mono- and multinucleated macrophages surrounding deposits of MSU crystals. Histologically, tophi consist of three zones: urate crystals in the central crystalline core, cellular corona in the middle zone, and fibrovascular tissue in the outer zone (29). In the present study, tophi were still present in both groups at 3 months. However, the tophi size decreased after effective ULT, which is consistent with previous studies (12-14). The results may be due to the surrounding fibrovascular tissue remaining despite the central crystal dissolution. The surrounding fibrovascular tissue may influence the US assessment of crystal dissolution in tophi.

A previous study has reported that bone erosion and destruction result from a granulomatous response (30). In the present study, cortical bone erosion appeared in three additional patients at 3 months, all of them with tophi at baseline. The results imply that the chronic inflammation surrounding tophi that contributes to bone erosion remained despite the tophi size reduction, consistent with the previous study (31).

Acute flare is caused by activation of the inflammasome complex by MSU crystals (32). ULT promotes the dissolution of MSU crystals, thereby reducing the inflammation they cause. In the present study, the power Doppler flow signal grade and synovium thickness at 3 months were lower than at baseline in both groups. Previous evidence has shown that the color Doppler flow signal is correlated with the histopathological findings of vascularity in the synovium (33). Therefore, synovium thickness decreases as the power Doppler flow signal grade decreases, which is consistent with the results of the present study. On the other hand, joint cavity effusion is associated with inflammation. At 3 months, it decreased to 6.7% of patients in the goal-not-achieved group and had disappeared in the goal-achieved group, which is consistent with the results mentioned above. As the degree of inflammation decreases, the pain will also decrease. Therefore, the VAS at 3 months was significantly lower than at baseline in both groups.

In the present study, only 25 (45.5%) patients achieved the target serum urate level at 3 months, which is less than in previous studies (12,13). This may be because the previous studies included 6 months of ULT, and the medication for ULT was different. It should be noted that the choice of medication depends on the physician, and it was not the focus of the present study.

In the present study, 13 patients (19.1%) receiving ULT did not persist for 3 months. To some extent, patients' impaired adherence may result from the fact that the change of crystals during ULT cannot be displayed intuitively. In our study, computer-aided MicroPure imaging showed a positive result. Therefore, we advise that computer-aided MicroPure imaging can be adopted to monitor aggregates dissolution during ULT, and it may encourage gouty patients adhere to ULT.

There were some limitations to the present study. First, joint aspiration, recognized as the reference for diagnosing gout, was not performed. It is invasive and often difficult due to a lack of fluid in the joint. Second, the sample size was relatively small, and a larger study is needed in the future to verify our results. Third, US cannot identify the chemical components of urate crystals due to technical limitations. As such, because all the patients enrolled in the present study were diagnosed with gout according to the ACR/EULAR criteria, all hyperechoic spots in the ROI could be considered as urate crystals. Identifying MSU crystals specifically with US may be a future research direction.

In conclusion, in comparison with B-mode US, computer-aided MicroPure imaging is a promising modality to sensitively and quantitatively monitor aggregate dissolution. The elementary lesion of the DCS and the power Doppler flow signal were decreased during effective ULT. In the present treat-to-target era, US combined with computer-aided MicroPure imaging may serve as a valuable tool in the management of patients with gout.

Acknowledgments

Funding: This work was supported in part by the National Natural Science Foundation of China (Grants 81671695, 81725008, 82001816, 82072092, and 81927801), the Shanghai Municipal Health Commission (Grants 2019LJ21 and SHSLCZDZK03502), and the Science and Technology Commission of Shanghai Municipality (Grants

19441903200, 18441905500 and 19DZ2251100).

Footnote

Reporting Checklist: The authors have completed the STROBE reporting checklist. Available at https://dx.doi.org/10.21037/atm-21-4059

Data Sharing Statement: Available at https://dx.doi.org/10.21037/atm-21-4059

Conflicts of Interest: All authors have completed the ICMJE uniform disclosure form (available at https://dx.doi.org/10.21037/atm-21-4059). The authors report that the present study was supported in part by the National Natural Science Foundation of China (Grants 81671695, 81725008, 82001816, 82072092, and 81927801), the Shanghai Municipal Health Commission (Grants 2019LJ21 and SHSLCZDZK03502), and the Science and Technology Commission of Shanghai Municipality (Grants 19441903200, 18441905500 and 19DZ2251100). The authors have no other conflicts of interest to declare.

Ethical Statement: The authors are accountable for all aspects of the work in ensuring that questions related to the accuracy or integrity of any part of the work are appropriately investigated and resolved. The cohort study was approved by the ethics committee of the Tenth People's Hospital Affiliated to Tongji University (Approval No.: SHSY-IEC-KY-4.0/18-170/01). Our database was prospectively established, and all patients provided informed consent. All procedures performed in this study involving human participants were in accordance with the Declaration of Helsinki (as revised in 2013).

References

1. Dalbeth N, Merriman TR, Stamp LK. Gout. Lancet 2016;388:2039-52.
2. Dehlin M, Jacobsson L, Roddy E. Global epidemiology of gout: prevalence, incidence, treatment patterns and risk factors. Nat Rev Rheumatol 2020;16:380-90.
3. Neogi T, Jansen TL, Dalbeth N, et al. 2015 Gout classification criteria: an American College of Rheumatology/European League Against Rheumatism collaborative initiative. Ann Rheum Dis 2015;74:1789-98.
4. Disveld IJM, Zoakman S, Jansen TLTA, et al. Crystal-proven gout patients have an increased mortality due to cardiovascular diseases, cancer, and infectious diseases especially when having tophi and/or high serum uric acid levels: a prospective cohort study. Clin Rheumatol 2019;38:1385-91.
5. Qaseem A, Harris RP, Forciea MA, et al. Management of Acute and Recurrent Gout: A Clinical Practice Guideline From the American College of Physicians. Ann Intern Med 2017;166:58-68.
6. Sundy JS, Baraf HS, Yood RA, et al. Efficacy and tolerability of pegloticase for the treatment of chronic gout in patients refractory to conventional treatment: two randomized controlled trials. JAMA 2011;306:711-20.
7. FitzGerald JD, Dalbeth N, Mikuls T, et al. 2020 American College of Rheumatology Guideline for the Management of Gout. Arthritis Rheumatol 2020;72:879-95.
8. Kuo CF, Grainge MJ, Mallen C, et al. Rising burden of gout in the UK but continuing suboptimal management: a nationwide population study. Ann Rheum Dis 2015;74:661-7.
9. Rashid N, Coburn BW, Wu YL, et al. Modifiable factors associated with allopurinol adherence and outcomes among patients with gout in an integrated healthcare system. J Rheumatol 2015;42:504-12.
10. Lee YH, Song GG. Diagnostic accuracy of ultrasound in patients with gout: A meta-analysis. Semin Arthritis Rheum 2018;47:703-9.
11. Terslev L, Gutierrez M, Schmidt WA, et al. Ultrasound as an Outcome Measure in Gout. A Validation Process by the OMERACT Ultrasound Working Group. J Rheumatol 2015;42:2177-81.
12. Ebstein E, Forien M, Norkuviene E, et al. Ultrasound evaluation in follow-up of urate-lowering therapy in gout: the USEFUL study. Rheumatology (Oxford) 2019;58:410-7.
13. Ottaviani S, Gill G, Aubrun A, et al. Ultrasound in gout: a useful tool for following urate-lowering therapy. Joint Bone Spine 2015;82:42-4.
14. Thiele RG, Schlesinger N. Ultrasonography shows

disappearance of monosodium urate crystal deposition on hyaline cartilage after sustained normouricemia is achieved. Rheumatol Int 2010;30:495-503.
15. Hammer HB, Karoliussen L, Terslev L, et al. Ultrasound shows rapid reduction of crystal depositions during a treat-to-target approach in gout patients: 12-month results from the NOR-Gout study. Ann Rheum Dis 2020;79:1500-5.
16. Christiansen SN, Østergaard M, Slot O, et al. Assessing the sensitivity to change of the OMERACT ultrasound structural gout lesions during urate-lowering therapy. RMD Open 2020;6:e001144.
17. Lu B, Lu Q, Huang B, et al. Risk factors of ultrasound-detected tophi in patients with gout. Clin Rheumatol 2020;39:1953-60.
18. Machado P, Eisenbrey JR, Cavanaugh B, et al. Microcalcifications versus artifacts: initial evaluation of a new ultrasound image processing technique to identify breast microcalcifications in a screening population. Ultrasound Med Biol 2014;40:2321-4.
19. Machado P, Eisenbrey JR, Stanczak M, et al. Characterization of Breast Microcalcifications Using a New Ultrasound Image-Processing Technique. J Ultrasound Med 2019;38:1733-8.
20. Yin L, Zhu J, Xue Q, et al. MicroPure imaging for the evaluation of microcalcifications in gouty arthritis involving the first metatarsophalangeal joint: a preliminary study. PLoS One 2014;9:e95743.
21. Keller SF, Lu N, Blumenthal KG, et al. Racial/ethnic variation and risk factors for allopurinol-associated severe cutaneous adverse reactions: a cohort study. Ann Rheum Dis 2018;77:1187-93.
22. Lu N, Rai SK, Terkeltaub R, et al. Racial disparities in the risk of Stevens-Johnson Syndrome and toxic epidermal necrolysis as urate-lowering drug adverse events in the United States. Semin Arthritis Rheum 2016;46:253-8.
23. Hui M, Carr A, Cameron S, et al. The British Society for Rheumatology Guideline for the Management of Gout. Rheumatology (Oxford) 2017;56:1056-9.
24. Martinoli C. Musculoskeletal ultrasound: technical guidelines. Insights Imaging 2010;1:99-141.
25. Gutierrez M, Schmidt WA, Thiele RG, et al. International Consensus for ultrasound lesions in gout: results of Delphi process and web-reliability exercise. Rheumatology (Oxford) 2015;54:1797-805.
26. Wang Q, Guo LH, Li XL, et al. Differentiating the acute phase of gout from the intercritical phase with ultrasound and quantitative shear wave elastography. Eur Radiol 2018;28:5316-27.
27. Ren WW, Li XL, Wang D, et al. Evaluation of shear wave elastography for differential diagnosis of breast lesions: A new qualitative analysis versus conventional quantitative analysis. Clin Hemorheol Microcirc 2018;69:425-36.
28. Peiteado D, Villalba A, Martín-Mola E, et al. Ultrasound sensitivity to changes in gout: a longitudinal study after two years of treatment. Clin Exp Rheumatol 2017;35:746-51.
29. Chhana A, Dalbeth N. The gouty tophus: a review. Curr Rheumatol Rep 2015;17:19.
30. Schlesinger N, Thiele RG. The pathogenesis of bone erosions in gouty arthritis. Ann Rheum Dis 2010;69:1907-12.
31. Wu M, Liu FJ, Chen J, et al. Prevalence and Factors Associated With Bone Erosion in Patients With Gout. Arthritis Care Res (Hoboken) 2019;71:1653-9.
32. Martinon F, Pétrilli V, Mayor A, et al. Gout-associated uric acid crystals activate the NALP3 inflammasome. Nature 2006;440:237-41.
33. Walther M, Harms H, Krenn V, et al. Correlation of power Doppler sonography with vascularity of the synovial tissue of the knee joint in patients with osteoarthritis and rheumatoid arthritis. Arthritis Rheum 2001;44:331-8.

Cite this article as: Wang Q, Bao H, Guo LH, Jin FS, Li XL, Yin HH, Yue WW, Zhu AQ, Wang LF, Sun LP, Xu HX. Quantitative assessment of crystal dissolution in gout during urate-lowering therapy with computer-aided MicroPure imaging: a cohort study. Ann Transl Med 2021;9(18):1444. doi: 10.21037/atm-21-4059

